

Author Query Form

Journal Title : JTC
Article Number : 426772

Dear Author/Editor,

Greetings, and thank you for publishing with SAGE Publications. Your article has been copyedited, and we have a few queries for you. Please address these queries when you send your proof corrections to the production editor. Thank you for your time and effort.

Please ensure that you have obtained and enclosed all necessary permissions for the reproduction of artistic works, (e.g. illustrations, photographs, charts, maps, other visual material, etc.) not owned by yourself, and ensure that the Contribution contains no unlawful statements and does not infringe any rights of others, and agree to indemnify the Publisher, SAGE Publications Ltd, against any claims in respect of the above warranties and that you agree that the Conditions of Publication form part of the Publishing Agreement.

Please assist us by clarifying the following queries:

No.	Query	Remarks
1	Please approve edits to the sentence ‘Incorporation of CNTs to the ...’	
2	Please approve edits to the sentence ‘TEM images were performed ...’	
3	Please approve edits to the sentence “Large differences between ...”	
4	Please define $ \eta^* $.	
5	Please update Ref 4 with volume and page range.	
6	Please check the year of publication in Ref 25.	
7	Please provide complete reference details in Ref 28.	
8	Please provide page range in Ref 38.	

Dielectric relaxation and rheological properties of single-walled carbon nanotubes reinforced poly(3-octylthiophene-2,5-diyl)

M. Abu-Abdeen^{1,2}, Ayman S. Ayesh¹ and A. A. Aljaafari¹

Abstract

Polymer nanocomposites consisting of single-walled carbon nanotubes (SWCNTs) and poly(3-octylthiophene-2,5-diyl) (P3OT) were prepared at different SWCNT loadings to investigate the influence of SWCNT content on the structure, dielectric and rheological properties of P3OT host. The dielectric parameters and dielectric relaxation behavior were investigated as a function of SWCNT loadings and frequency. Dielectric results reveal that SWCNTs enhance the polar character of P3OT host, shift the peak maximum of loss tangent toward higher frequency values and increase the alternating current conductivity especially above the percolation threshold point. Besides, the rheological properties of SWCNT-P3OT composites were also investigated to realize the effect of SWCNT content on the complex viscosity, storage and loss moduli at different frequency values. The obtained results reveal that nanocomposites become electrically percolated at 0.44 wt% SWCNTs, while the rheological percolation threshold was found at 0.5 wt%. Additionally, this study showed that the relaxation behavior in SWCNT-P3OT composites is mainly due to the viscoelastic relaxation process. Moreover, at high level of SWCNT loadings, the nanotubes became more interconnected to form network like structures in the P3OT host. Finally, results obtained from structure–property analysis reveal that the addition of SWCNTs to P3OT host reduced the vibrational

¹ Department of Physics, College of Science, King Faisal University, Al-Ahsa, Saudi Arabia

² Department of Physics, College of Science, Cairo University, Egypt

Corresponding author:

M. Abu-Abdeen, Department of Physics, College of Science, King Faisal University, P.O. B 400, 31982 Al-Ahsa, Saudi Arabia

Email: mmaabdeen@yahoo.com

freedom of the polymer chains as a consequence of the intercalation of the polymer matrix into the nanotubes.

Keywords

conjugated polymers, dielectric properties, rheological properties

Introduction

Carbon nanotubes (CNTs) have attracted considerable attention on account of their excellent mechanical, electrical and thermal properties. Therefore, they offer many opportunities for the development of novel material systems.^{1,2} Many methods have been reported for synthesizing CNTs.^{1,3} Currently, CNT growth processes, such as chemical vapor deposition (CVD), are based on the use of transition metal catalysts. CNT synthesis by CVD is a promising route for the bulk production of high-purity CNTs suitable for commercialization.^{1,3}

Conjugated polymers can become electrically conducting by doping or oxidation process but are usually insoluble in common solvents. One method to convert them into soluble is to add lateral groups to the backbone of the molecules, such as the case of poly(3-octylthiophene-2,5-diyl) (P3OT). However, conducting polymers generally exhibit an alternating single bond–double bond structure (conjugation) based on sp²-hybridized carbon atoms. This leads to a highly delocalized π -electron system with large electronic polarizability. This enables both absorption within the visible light region, due to π - π transitions between the bonding and antibonding pz orbitals, and electrical charge transport—two requirements that need to be met by semiconductors for power generation in solar cells. Using conjugated polymers to fabricate optoelectronic devices, such as organic light-emitting diodes (OLEDs), organic field-effect transistors (OFETs) and organic solar cells (OSCs), is attractive because of their unique processability from solution.^{3–5}

Nanocomposite materials made out of polymers and CNTs offer the promise of plastic composites with enhanced structural, electrical, mechanical and thermal properties.^{6,7} Accordingly, in the recent years, much attention has been paid to the use of nanotubes in composite materials, to harness their exceptional electronic and mechanical properties.

Polymer-CNT composites have shown a lot of potential for a vast range of applications, including solar cells, diodes and so on. Additionally, a wide range of host materials has been used, including polymers.⁷ Most recently, research has focused on the composites of electronically active conjugated polymers and CNTs, which demonstrate a number of advantages. Incorporation of CNTs into the conjugated polymers shows potential for electronic device applications, promising to greatly enhance transport properties in these systems. This is thought to be a key issue for the realization of viable devices such as OLEDs and solar cells.^{2,4–14} Besides, the physical properties such as electrical, mechanical, optical and structural properties of CNT-P3OT composites were recently studied by many researchers.^{7,14–19} However, this study will introduce an important

addition in the dielectric relaxation behavior and rheological properties of CNT-P3OT composites.

Toward the aim of the present work, this research focused on the effect of single-walled carbon nanotubes (SWCNTs) on the structure, dielectric and rheological properties of the P3OT host at different SWCNT loadings. The dielectric relaxation, alternating current (ac) conductivity, impedance and loss tangent for these composites are presented, analyzed and discussed. The complex viscosity, storage modulus and loss modulus will also be investigated. Correlations between structure, dielectric and rheological properties are also discussed.

Experimental

CNT preparation

SWCNTs were grown via the alcohol catalytic chemical vapor deposition (ACCVD) technique. Cobalt acetate-supported catalyst was placed in alumina combustion boat; whereas a 10° inclined graphite stage was used to support the substrates and the group was then placed at the center of a tube furnace. The tube was evacuated to 20 Pa, and the samples were heated to the desired reaction temperature under $1.67 \times 10^{-8} \text{ m}^3/\text{s}$ of flowing argon. Once the growth temperature was reached (800°C), the samples were held at that temperature for 5 min. The argon was then shut off and the tube was evacuated before the introduction of alcohol vapor. The alcohol vapor (ethanol) was then transferred into the tube furnace to achieve a pressure of 666–1333.2 Pa. The alcohol flow rate in the growth chamber was controlled by controlling the alcohol bath temperature. After growth, the alcohol vapor was evacuated, argon was introduced again and the reaction tube was cooled to room temperature. CNTs growth time was kept constant at 50 min. The blackened catalysts were then sonicated for 2 h in chloroform. Few milligrams of SWCNTs were collected after the evaporation of chloroform for using in applications. More details of such synthesis can be found elsewhere.²⁰ X-ray diffraction (XRD) and transmission electron microscope (TEM) results revealed that the synthesized CNTs were bundles of SWCNTs as shown in Figure 1, with average diameter of 1.6 nm.^{21,22}

Films preparation

P3OT was purchased from Aldrich (Ref. No. 445711). It has more than 98.5% head-to-tail regiospecific conformation, molecular weight 34,000, melting point 90°C and fluorescence $\lambda_{\text{excitation}}$ 442 nm; $\lambda_{\text{emission}}$ 562 nm in chloroform.

P3OT was dissolved in chloroform by ultrasonication for 30 min. At same time, the required amount of CNTs was dispersed again in chloroform and sonicated for 30 min to obtain dispersed nanotube suspension. Both solutions were mixed together and further sonicated for 2 h to obtain a well-dispersed homogenous SWCNT-P3OT solution without any detectable solid precipitations. The resulting solution was poured to a completely horizontal glass petri dish and then dried at room temperature. Finally, the dried film was heated up to 50°C to remove the remnant solvent. A series of composite films were

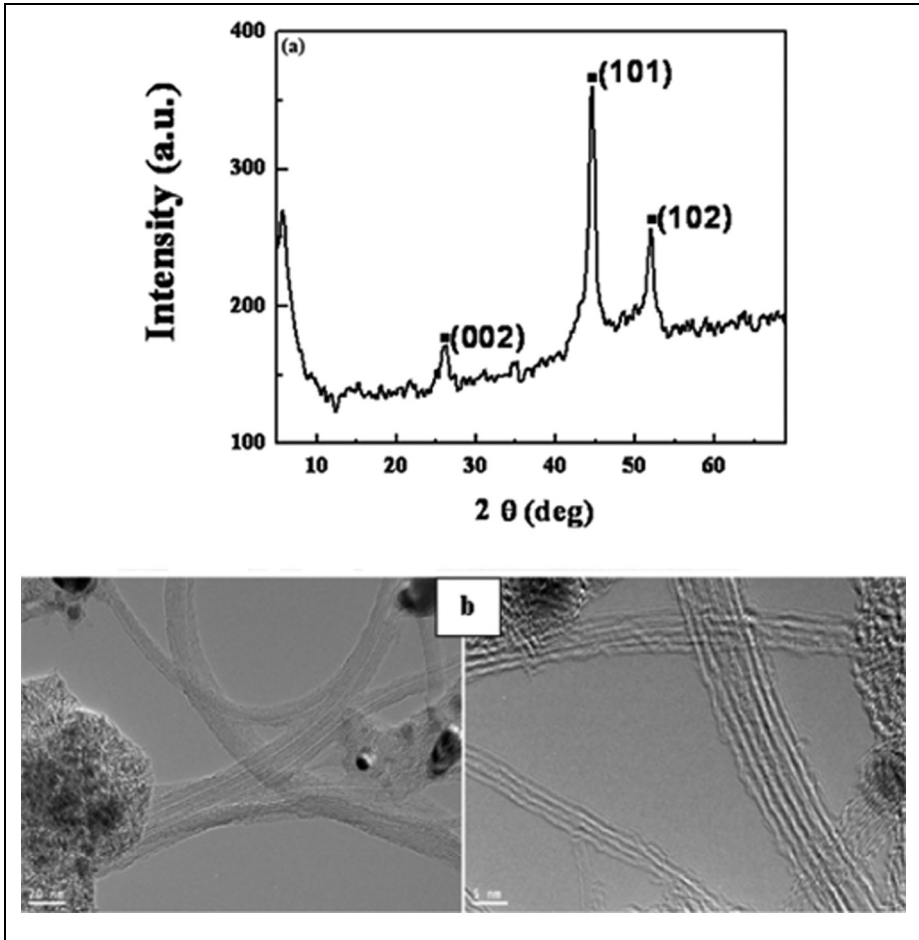


Figure 1. (a) Typical X-ray diffraction (XRD) pattern for synthesized carbon nanotubes (CNTs). (b) Transmission electron microscopic (TEM) image of synthesized CNTs on Si substrate at 800°C .

prepared at different weight ratios (0–5 wt%) of SWCNT-P3OT under same preparation conditions.

X-ray diffraction and transmission electron microscope

X-ray diffractions were measured at room temperature with the current and voltage operating at 40 mA and 45 kV, respectively. The X-ray beam was $\text{Cu K}\alpha$ ($\lambda = 0.15406 \text{ nm}$) radiation from a sealed tube operating at a voltage of 45 kV and a current of 40 mA. The samples were scanned in the 2θ range of 5° – 70° , with a step scan mode (or step size) of 0.001° .

TEM images were performed on a JEM Model 1011 at 100 kV held in KACST, Saudi Arabia. Furthermore, nanotubes grown in the powder form were sonicated in methanol and placed on holey/lacey carbon-coated copper grids.

Dielectric measurements

Dielectric measurements were carried out using precision 4294A impedance analyzer (Agilent technologies) over a frequency range of 40 Hz–10 MHz at room temperature. The loss tangent, $\tan \delta$, relative permittivity, ϵ' , dielectric loss, ϵ'' , real part of impedance, Z_r and imaginary part of impedance, Z_i , were obtained directly from the bridge. Calibration (short and open) of the impedance analyzer was done before the measurements. Disk-shaped specimens were cut from the SWCNT-P3OT composite sheets and placed between two copper plates (10 mm diameter) of a test sample holder placed in a shielded cell designed for this purpose. The two leads of the holder were connected to the terminals of the impedance analyzer. The measurements were carried out three times to ensure reproducibility of the results. The ac conductivity, σ_{AC} , was calculated using the following equation²³:

$$\sigma_{AC} = \omega \epsilon'' \epsilon_o = 2\pi f \epsilon'' \epsilon_o \quad (1)$$

where ϵ_o is the permittivity of free space ($8.85 \times 10^{-12} \text{ Fm}^{-1}$) and f is the frequency (Hz).

Rheological properties

Rheological tests were carried out on a DMA Q800 machine TA instruments (USA), using the tension film clamping arrangement at a force of 0.5 N and strain amplitude of oscillation 15 μm at an isothermal process of 25°C. Specimens in the form of films with dimensions 15 mm length, 4 mm width and 0.1 mm thick were used.

Results and discussion

X-ray diffraction

Figure 2 illustrates the XRD patterns of SWCNT-P3OT composites. The reflection peak (1 0 0) represents the a axis and it corresponds to in-plane interchain distance. Besides, an amorphous halo wide-angle peak with lesser intensity appears at $2\theta = 23.6$ with a d spacing of 4.18 Å, which represents the stacking distance of the thiophene rings or interplanar distance.⁴ There is no significant change in the scattering peaks' positions with the addition of SWNT with respect to interplane and intrachain distances. Furthermore, it is clear that the peak height of the (1 0 0) and (2 0 0) planes decreases with SWCNTs. The lower peak heights for the P3OT loaded with SWCNTs especially at high loading level could be attributed to the entropy-driven disorder due to a higher mobility of the polymer backbone within the side-chain matrix.²⁴ Additionally, the average crystallite size of SWCNT-P3OT composites was calculated at peak positions, $2\theta = 8.73$ and 13.10 using the Debye–Scherrer formula²⁵

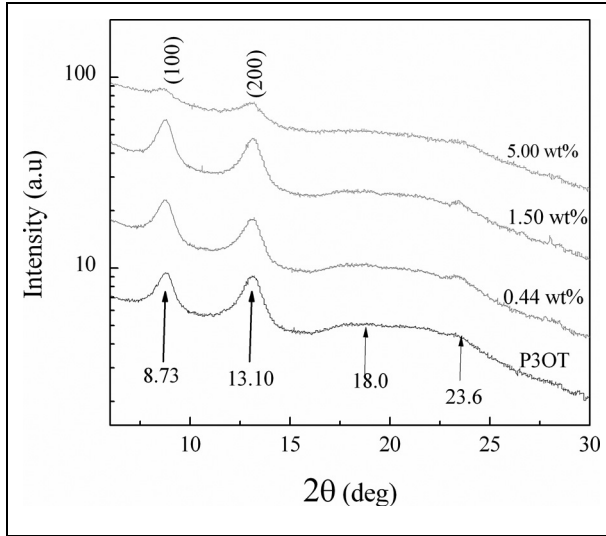


Figure 2. X-ray diffraction (XRD) patterns of single-walled carbon nanotube–poly(3-octylthiophene-2,5-diyl) (SWCNT-P3OT) composites.

$$D = \frac{K\lambda}{\beta \cos(\theta)} \quad (2)$$

where D is the crystallite size, λ is the wavelength of the X-ray radiation, K is usually taken as 0.89, 2θ is the Bragg angle of the reflected peak, and β is the peak width at half-maximum height. The obtained results together with d-spacing results are listed in Table 1. It is clear that the addition of SWCNTs to P3OT host increases the values of crystallite size.

From the above results, one can say that SWCNTs narrow the crystalline regions and at the same time increases their ordered length.^{4,24} This, however, also supports the idea that as the SWCNT content increases, the interconnections between nanotubes increase and consequently will lead to the formation of a network-like structure especially at high level of SWCNT content. Other factor may also contribute to the above changes, that is the physical wrapping of the polymer on the walls of the nanotubes.^{4,26}

Dielectric properties and dielectric relaxation behavior

Relative permittivity ϵ' , dielectric loss ϵ'' , loss tangent $\tan \delta$, real part of impedance Z_r and imaginary part of impedance Z_i data were collected directly from the impedance meter at room temperature at the frequency range of 40 Hz–10 MHz for SWCNT/P3OT composites. The ac conductivity σ_{AC} was calculated from the well-known collected data in accordance to Eq. (1). The obtained results are presented graphically in Figures 3–7. It is clear that relative permittivity and ac conductivity are increased with increase in the

Table 1. XRD parameters for SWCNT-P3OT composites

System	Peak position (2θ)	d-spacing (\AA)	Crystallite size (\AA)
P3OT	8.73	11.2434	1.18
	13.10	7.5001	1.18
	18.00	5.4670	
	23.60	4.1797	
SWCNT (0.44%)	8.73	11.2434	1.32
	13.10	7.5001	1.25
	18.00	5.4670	
	23.60	4.1797	
SWCNT (1.5%)	8.73	11.2434	1.51
	13.10	7.5001	1.31
	18.00	5.4670	
	23.60	4.1797	
SWCNT (5%)	8.73	11.2434	2.04
	13.10	7.5001	1.40
	18.00	5.4670	
	23.60	4.1797	

P3OT: poly(3-octylthiophene-2,5-diyl), SWCNTs: single-walled carbon nanotubes, XRD: X-ray diffraction.

loadings of SWCNTs in the P3OT host while impedance is decreased. Besides, the decrease in relative permittivity with frequency could be attributed to the insufficient time for dipoles to align before the field changes direction.^{23,27,28} The variations in relative permittivity, ac conductivity and impedance with SWCNTs loadings could be attributed to the ion charge diffusions and orientational polarizations in addition to the contribution of Maxwell–Wagner polarization.^{26–29} However, it is clear that SWCNTs increase the polar character of the P3OT host.

The ac conductivity versus SWCNTs loading is shown in Figure 8 at low- and high-frequency value. It is very clear that the percolation threshold is around 0.44%, and this behavior appears to be independent of the frequency values.

In Figure 4, loss tangent curves show a single relaxation peak (α -relaxation). It is also clear that the peak maximum shifts isothermally toward higher frequency values and the value of loss tangent at the peak maximum decreases with SWCNTs especially above the percolation threshold. The same variations can also be seen in the case impedance. This, however, could be attributed to the reduction in the vibrational freedom of the polymer chains as a consequence of the intercalation of the polymer matrix with the nanotubes.^{7,14} There is good agreement between the results obtained from the dielectric and those obtained from XRD such that both of them lead to one conclusion that is increase in SWCNT content in P3OT will lead to increased physical wrapping of the polymer on the walls of the nanotubes and reduced vibrational freedom of the polymer chains. On the other hand, in the present work we will also introduce an important addition in the dielectric relaxation behavior of SWCNT/P3OT composites in the next paragraph.

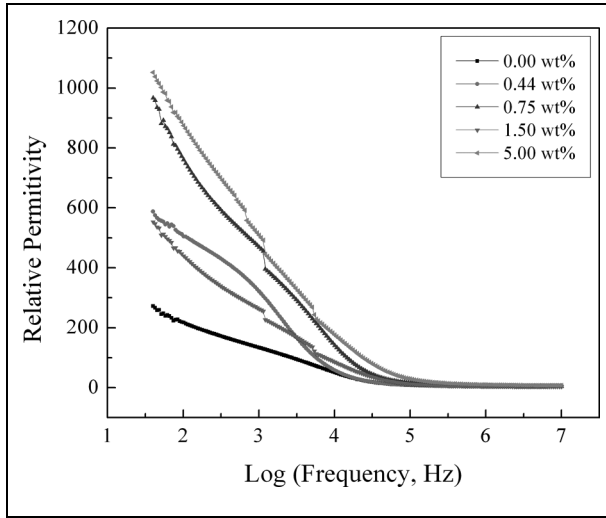


Figure 3. Relative dielectric permittivity versus log(frequency) for single-walled carbon nanotube–poly(3-octylthiophene-2,5-diyl) (SWCNT-P3OT) composites.

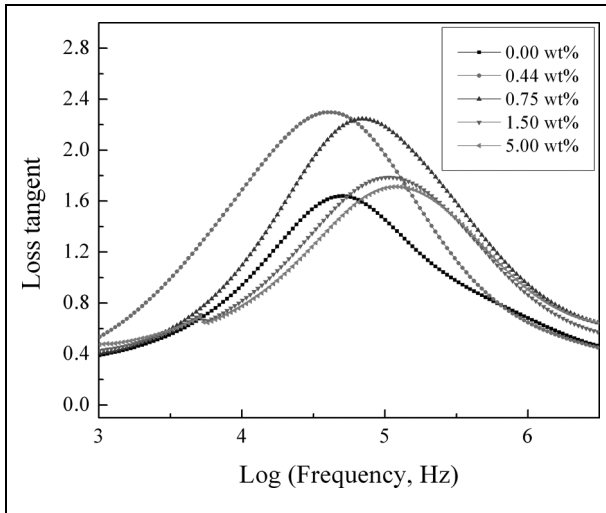


Figure 4. Loss tangent versus log(frequency) for single-walled carbon nanotube–poly(3-octylthiophene-2,5-diyl) (SWCNT-P3OT) composites.

It was reported previously^{23,26,27} that if the Argand plot between imaginary part (M'') versus real part (M') of electric modulus has semicircular behavior then the relaxation is due to conductivity relaxation process; if not, then it is due to viscoelastic relaxation (or

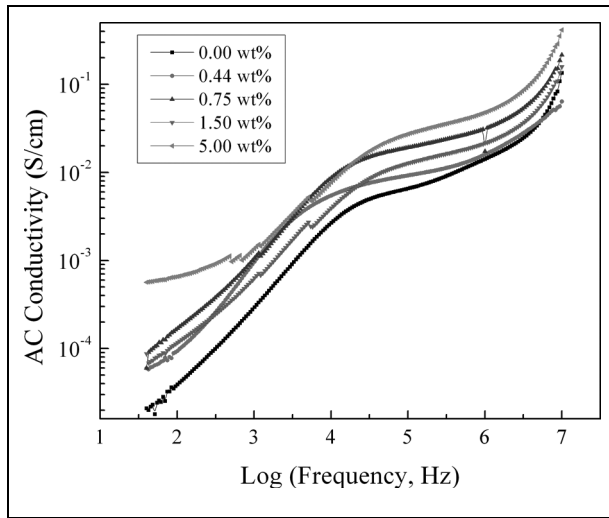


Figure 5. The alternating current (ac) conductivity versus log(frequency) for single-walled carbon nanotube (SWCNT-P3OT) composites.

polymer molecular relaxation). In the present work, the values of M' and M'' were determined from

$$M^* = \frac{1}{\epsilon^*} = \frac{1}{\epsilon' - i\epsilon''} = \frac{\epsilon' + i\epsilon''}{(\epsilon' - i\epsilon'')(\epsilon' + i\epsilon'')}$$

$$M^* = \frac{\epsilon'}{(\epsilon' - i\epsilon'')(\epsilon' + i\epsilon'')} + i \frac{\epsilon''}{(\epsilon' - i\epsilon'')(\epsilon' + i\epsilon'')}$$

$$M^* = \frac{\epsilon'}{(\epsilon'^2 + \epsilon''^2)} + i \frac{\epsilon''}{(\epsilon'^2 + \epsilon''^2)} = M' + iM'' \tag{3}$$

Where ϵ' is the permittivity, ϵ'' is the dielectric loss, M' is the electric modulus and M'' is the electric loss modulus. Large differences between the properties of viscoelastic relaxations and the properties of conductivity relaxations are observed in the polymers. The obtained results are presented graphically in Figure 9. It is clear that all plots do not follow the semicircular behavior. This indicates that, at the domain frequency range, the relaxation process is due to viscoelastic relaxation process.^{23,26,27}

3

Rheological properties

The rheological properties of SWCNT-P3OT composites were also investigated at room temperature and the domain frequency range. The complex viscosity as a function of the angular frequency is shown in Figure 10. Apparently, SWCNTs have a crucial effect on the rheological behavior of the composites, even at low loadings. The complex viscosity

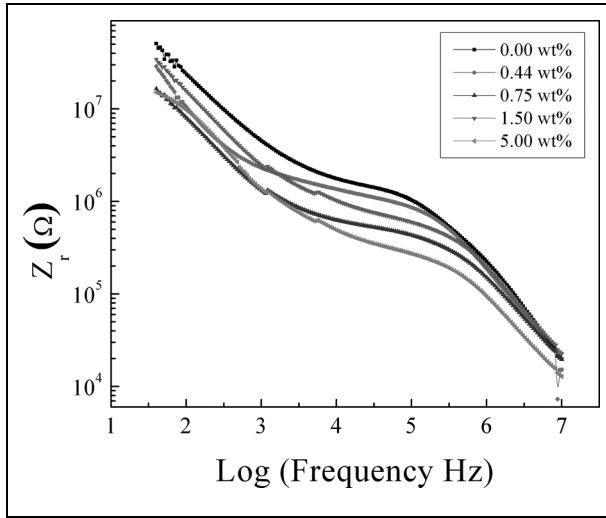


Figure 6. Real part impedance versus log(frequency) for single-walled carbon nanotube–poly(3-octylthiophene-2,5-diyl) (SWCNT-P3OT) composites.

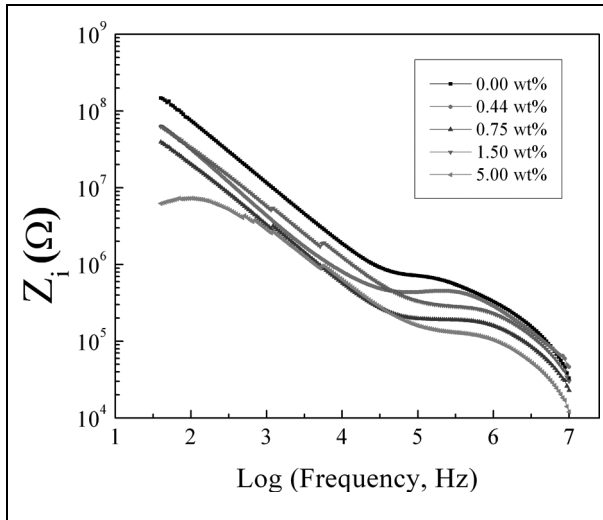


Figure 7. Imaginary part impedance versus log(frequency) for single-walled carbon nanotube–poly(3-octylthiophene-2,5-diyl) (SWCNT-P3OT) composites.

increases with increasing CNT content in the entire frequency range but is more pronounced at low frequencies. At high frequencies, the impact of the CNTs on the rheological properties is definitely weaker, which suggests that the nanotubes do not significantly influence the short-range dynamics of the polymer chains. Generally, CNTs

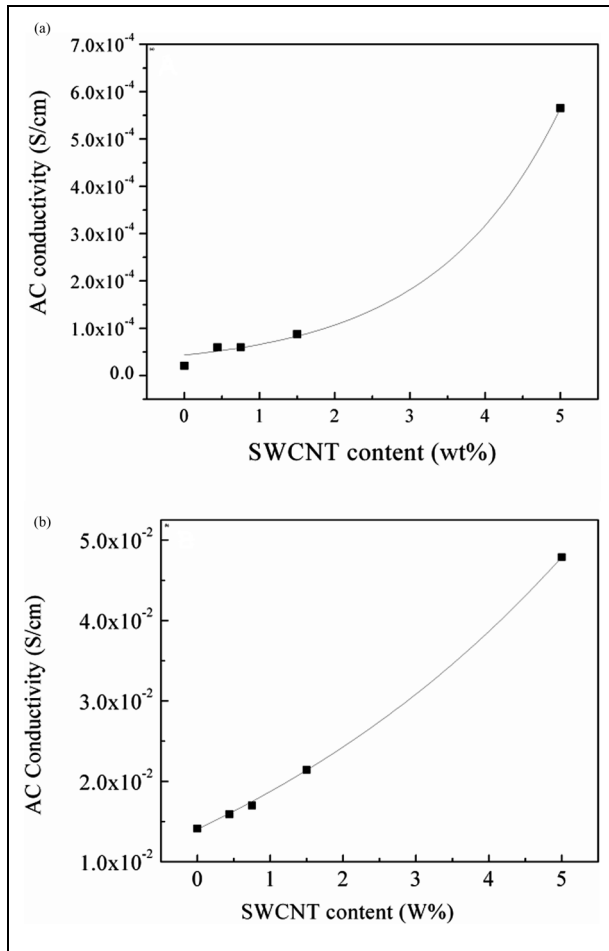


Figure 8. (a) Alternating current (ac) conductivity versus single-walled carbon nanotube (SWCNT) concentration (wt%) at 40 Hz. (b) ac conductivity versus SWCNT concentration (wt%) at 1 MHz.

do affect polymer chain relaxation but with little effect on the local motion at short ranges.³⁰ The decrease in the complex viscosity with increasing frequency indicates a non-Newtonian behavior over the frequency range investigated. The shear thinning behavior observed in the SWCNT-P3OT nanocomposites may be attributed to the orientation of the rigid molecular chains in the nanocomposites during the applied force. The effect of SWCNTs on $|\eta^*|$ of the studied nanocomposites is more significant at low frequency compared with high frequency, and this effect was reduced with increasing frequency because of the strong shear thinning behavior induced by incorporating CNT.

The variation in $|\eta^*|$ of the SWCNT-P3OT nanocomposites with the SWCNT content at different frequencies is shown in Figure 11. It can be seen that the $|\eta^*|$ of the

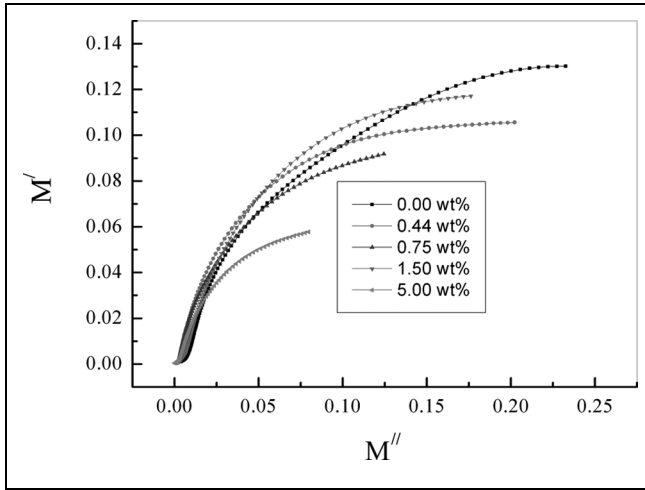


Figure 9. Argand plots of single-walled carbon nanotube–poly(3-octylthiophene-2,5-diyl) (SWCNT-P3OT) composites.

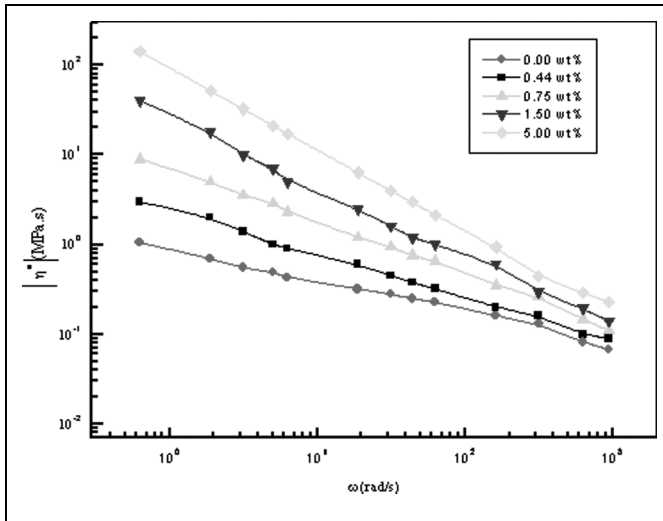


Figure 10. Complex viscosity of single-walled carbon nanotubes–poly(3-octylthiophene-2,5-diyl) (SWCNT-P3OT) composites as a function of the angular frequency.

nanocomposites increased with increasing CNT content over the frequency ranges investigated. In addition, the extent of increase in the $|\eta^*|$ with increasing SWCNT content was more pronounced at low frequency compared with that at high frequency. This increase in $|\eta^*|$ with increasing SWCNT content may be attributed to the increase in

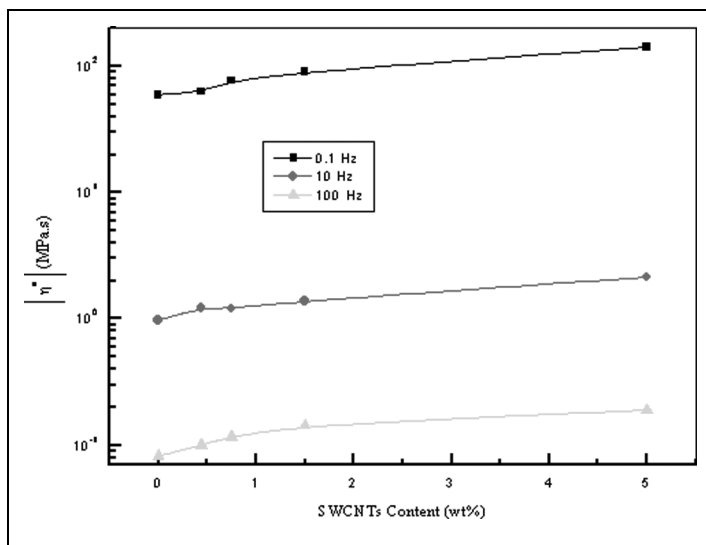


Figure 11. Variation in the complex viscosity of single-walled carbon nanotube–poly(3-octylthiophene-2,5-diyl) (SWCNT-P3OT) nanocomposites with SWCNT content at different frequencies.

physical interactions between the P3OT matrix and the SWCNTs with high aspect ratio and large surface area. The increase in $|\eta^*|$ of the SWCNT-P3OT nanocomposites with the SWCNTs was closely related to the increase in the storage modulus, which will be described in the following section. Now there are strong evidences from XRD, dielectric and rheological results that the increase in SWCNT content of P3OT host will lead to the increase in the physical wrapping of polymer chains around the nanotubes and decrease the degree of vibrational freedom of polymer chains.

The complex viscosity can be expressed by a power law $|\eta^*| \propto \omega^{-\beta}$. The values of β are presented in Figure 12a as a function of the SWCNT content.

The storage modulus G' and loss modulus G'' of the SWCNT-P3OT nanocomposites as a function of frequency are shown in Figure 13. The values of G' and G'' of the SWCNT-P3OT nanocomposites increase with increasing frequency and SWCNT content, this increment being more significant at low frequency. This rheological response is similar to the relaxation behavior of the typical filled-polymer composite systems.³¹ It is known that the polymer chains are fully relaxed and exhibit characteristic homopolymer-like terminal flow behavior, resulting in the flow curves of polymers being expressed by the power law $G' \propto \omega^2$ and $G'' \propto \omega$.^{31–33} Krishnamoorti and Giannelis,³⁴ reported that the slopes of $G'(\omega)$ and $G''(\omega)$ for polymer/layered silicate nanocomposite were much smaller than 2 and 1, respectively, which are the values expected for linear homodispersed polymer melts. They suggested that large deviations in the presence of a small quantity of layered silicate might be due to the formation of a network structure in the molten state.

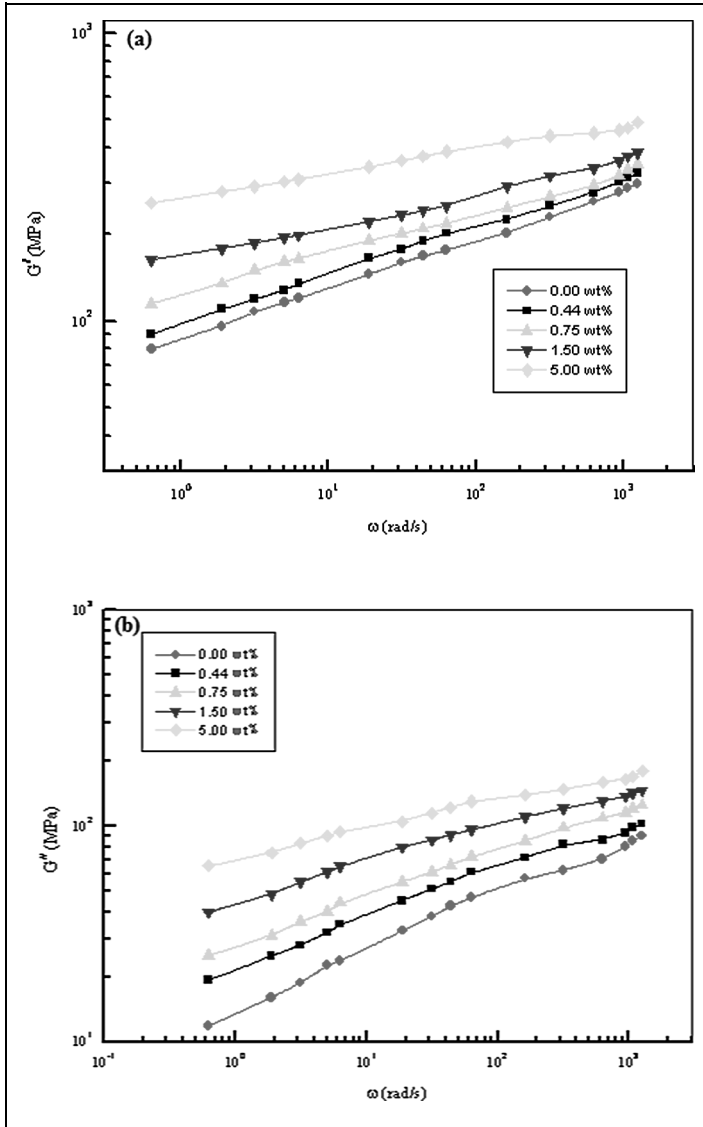


Figure 12. (a) Slopes β of $|\eta^*|$ for single-walled carbon nanotube–poly(3-octylthiophene-2,5-diyl) (SWCNT-P3OT) nanocomposites. (b) Slopes α and γ of $G'(\omega)$ and $G''(\omega)$ for single-walled carbon nanotube–poly(3-octylthiophene-2,5-diyl) (SWCNT-P3OT) nanocomposites.

The complex viscosity can be expressed by a power law $|\eta^*| \propto \omega^{-\beta}$. The dependence of the values of β on the concentration of SWCNT content is presented in Figure 12a as a function of the SWCNT content. Besides, the dependence of $G'(\omega)$ and $G''(\omega)$ for SWCNT-P3OT nanocomposites can be expressed by power laws of the forms $G'(\omega) \propto \omega^\alpha$

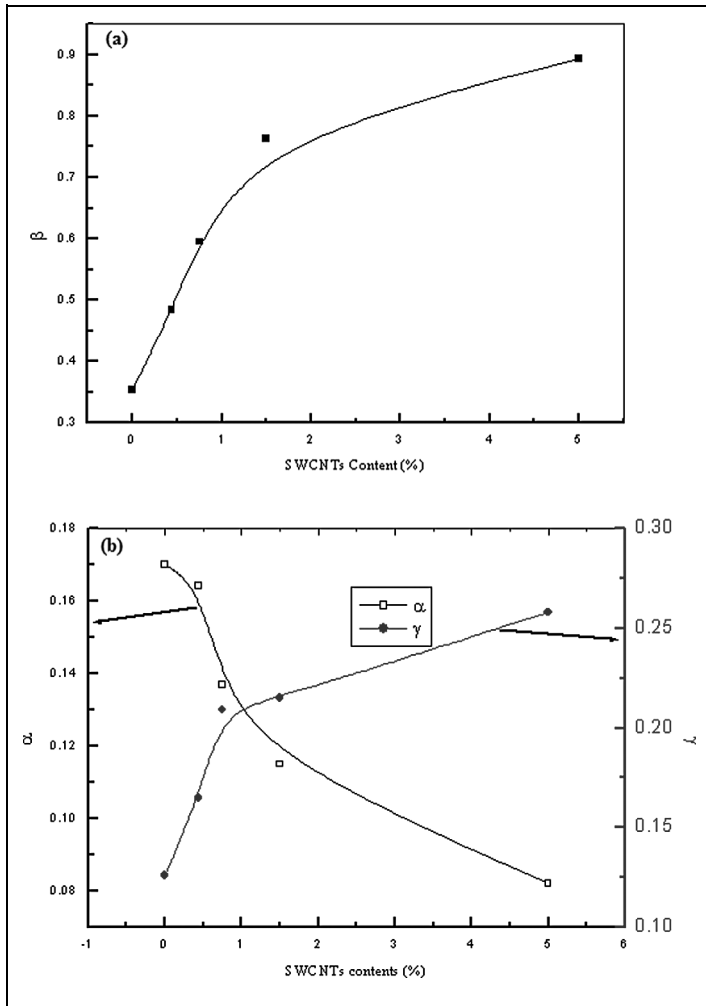


Figure 13. (a) Variation in the storage modulus of single-walled carbon nanotube–poly(3-octylthiophene-2,5-diyl) (SWCNT-P3OT) nanocomposites with different SWCNT content, as a function of frequency. (b) Variation in the loss modulus of SWCNT-P3OT nanocomposites with different SWCNT content, as a function of frequency.

and $G''(\omega)\alpha\omega^\gamma$, with the values of α and γ presented in Figure 12b. These values indicate the nonterminal behavior with the power-law dependence for G' and G'' of the SWCNT-P3OT nanocomposites.

Similar nonterminal rheological behavior has been observed in ordered block copolymers and smectic liquid–crystalline small molecules.^{35–37} The decrease in the slope of G' (and the increase in the slope of G'') for the SWCNT-P3OT nanocomposites with

increasing SWCNT content may be explained by the fact that the nanotube–nanotube interactions increased with increasing CNT content and led to the formation of the interconnected or network-like structures of SWCNTs in the polymer nanocomposites, resulting in the pseudo–solid-like behavior.

The variation in the storage modulus and loss modulus of the SWCNT-P3OT nanocomposites with the SWCNT content at different frequencies is shown in Figure 14. It can be seen that the incorporation of small quantity of SWCNTs (0.75 wt%) into the P3OT matrix unchanged the values of G'' for the SWCNT-P3OT nanocomposites over the frequency range investigated, except for the results measured at a frequency of 0.1 Hz. This phenomenon may be attributed to the formation of the viscous surface layers around the dispersed nanotubes leading to an increase in the free volume in this nanocomposite system, making it easier for flow to occur.³⁸ As SWCNT content increased, the physical interactions between the nanotubes may lead to the formation of interconnected or network-like structure of the nanotubes in the polymer matrix.³⁹ Besides, the extent of the increase in G' of the SWCNT-P3OT nanocomposites is higher than that of G'' over the frequency range investigated. In addition, the storage modulus and loss modulus of the SWCNT-P3OT nanocomposites were significantly improved relative to the P3OT matrix.

Rheological percolation threshold of CNT/polymer composites

Transition from viscoelastic properties exhibiting liquid-like characteristics to pseudo–solid-like behavior can be expressed by the rheological percolation threshold. To determine the rheological percolation threshold of CNTs-polymer composites, the relations between rheological quantities and the concentration of the filler in a medium are drawn into two modified power law equations^{30,37,40,41}:

$$\eta^* \alpha (m - m_c)^a \quad (4)$$

$$G' \alpha (m - m_c)^t \quad (5)$$

where, m is the loading of CNTs, m_c the rheological percolation threshold, a and t are the critical exponents that are dependent on the oscillatory frequency. The percolation theory predicts that $a = t \sim 2$ in three dimensions³⁰; however, as it is explained in the next paragraph, the rheological percolation threshold does not relate to the geometrical percolation threshold (where the physical contact between particles is assumed). Thus, this fitting parameter may significantly vary from the expected theoretical value.

In percolated systems, one can observe a drastic change in the storage modulus and viscosity at a fixed frequency for a given concentration of the filler. This indicates that the CNT-polymer composite reaches a rheological percolation threshold at which the nanotubes block the motion of the polymer molecules. Such a conclusion can be also clearly observed if one refers to Figure 4, where it can be observed that the peak maximum of loss tangent in case of 0.44% SWCNT shifts slightly toward lower frequency. This indicates that CNT at the percolation threshold restricts the chain mobility.

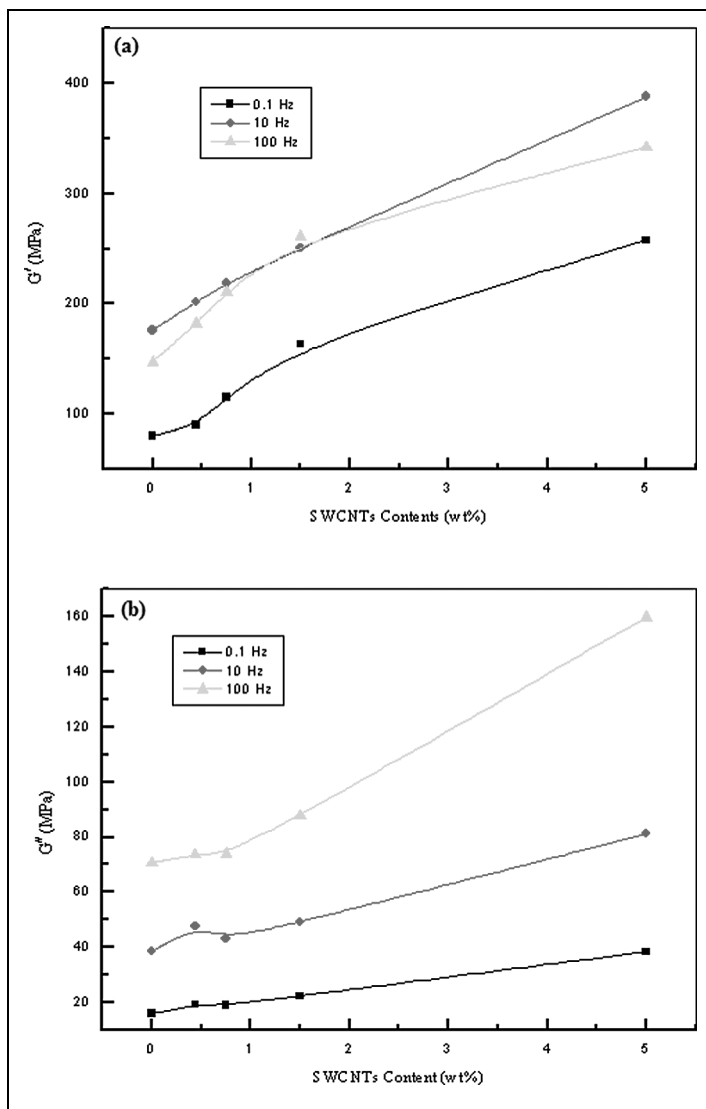


Figure 14. (a) Storage modulus of single-walled carbon nanotube–poly(3-octylthiophene-2,5-diyl) (SWCNT-P3OT) nanocomposites at different frequencies, as a function of SWCNT content. (b) Loss modulus of SWCNT-P3OT nanocomposites at different frequencies, as a function of SWCNT content.

The rheological percolation threshold has also been shown to be temperature dependent, which is in contrast to the assumption that the liquid–solid transition originates only from the network formation of the filler.⁴² This reveals that rheology reflects a combined network of the polymer chains and nanotubes, not only the interconnection

between CNTs. The entangled nanotube–polymer network dominates the rheological properties of the composites.⁴¹

In this study, the power law Eqs. (4) and (5) were used to determine the value of the rheological percolation threshold. The functions were fitted to the experimental data points of $|\eta^*|$ and G' at 0.1 Hz for $m > m_c$ (concentrations above percolation threshold). Figure 15 shows the complex viscosity and storage modulus as a function of SWCNT content at 0.1 Hz.

The scaling parameters were found by incrementally varying m_c until the best linear fit to the data points was obtained (with the best achieved, optimal value of correlation coefficient R). The rheological percolation threshold (m_c) was found to be at the SWCNT concentrations of 0.5 wt%. Scaling exponents, $a = 0.283$ and $t = 0.356$, differ from the theoretical value of the percolating systems in three dimensions ($a = t \sim 2.0$). The rheological percolation threshold does not refer to the geometrical percolation, where the filler forms interconnected paths along the entire composite, which is considered in theoretical studies. The low rheological percolation threshold obtained in this study is attributed not only to the high aspect ratio of the CNT filler but also to the good and homogenous dispersion of SWCNTs within the P3OT matrix.

There are many factors that may affect the viscoelastic response of the samples, including the molecular weight of polymers, their morphology, degree of dispersion of nanotubes in the matrix, aspect ratio of the filler, alignment of CNTs (which diminishes the formation of percolated network) and temperature.^{30,42} On this basis, it is difficult to compare the percolation threshold found in this study (0.5 wt%) to earlier reported values of diverse materials ranging from 0.1 to 5 wt%.^{30,40–42} Nevertheless, a percolation threshold at 0.5 wt% is fairly low and opens up possibilities for the formation of a new class of polymeric composites with advanced mechanical properties at a low-weight fraction of nanotubes. Further improvement in the composite fabrication techniques, together with high aspect ratio of nanotubes, can permit the formation of percolated structures even at a lower load of the filler. This is a simple guideline for the modification of the polymeric structures with a modest amount of CNTs but resulting in significant changes in the properties.

Conclusions

CNTs are synthesized using ACCVD techniques. The XRD results and TEM images reveal that CNTs synthesized at 800°C are mainly SWCNTs. SWCNT-P3OT composites were prepared at different loadings to investigate the effect of SWCNT loadings on the structure, dielectric properties, dielectric relaxation behavior and rheological properties of the P3OT host. The structural analysis of SWCNT-P3OT composites is also considered using XRD. XRD results reveal that the addition of SWCNTs to P3OT host narrows the crystalline regions and increases their ordered length. On the other hand, dielectric spectroscopy results indicate that SWCNTs enhance the polar character of P3OT host and also increase the ac conductivity. The ac conductivity results show that the network of SWCNT-P3OT system are percolated at 0.44 wt% SWCNTs which appear to be independent of the frequency. Furthermore, a single relaxation peak (α -relaxation) is

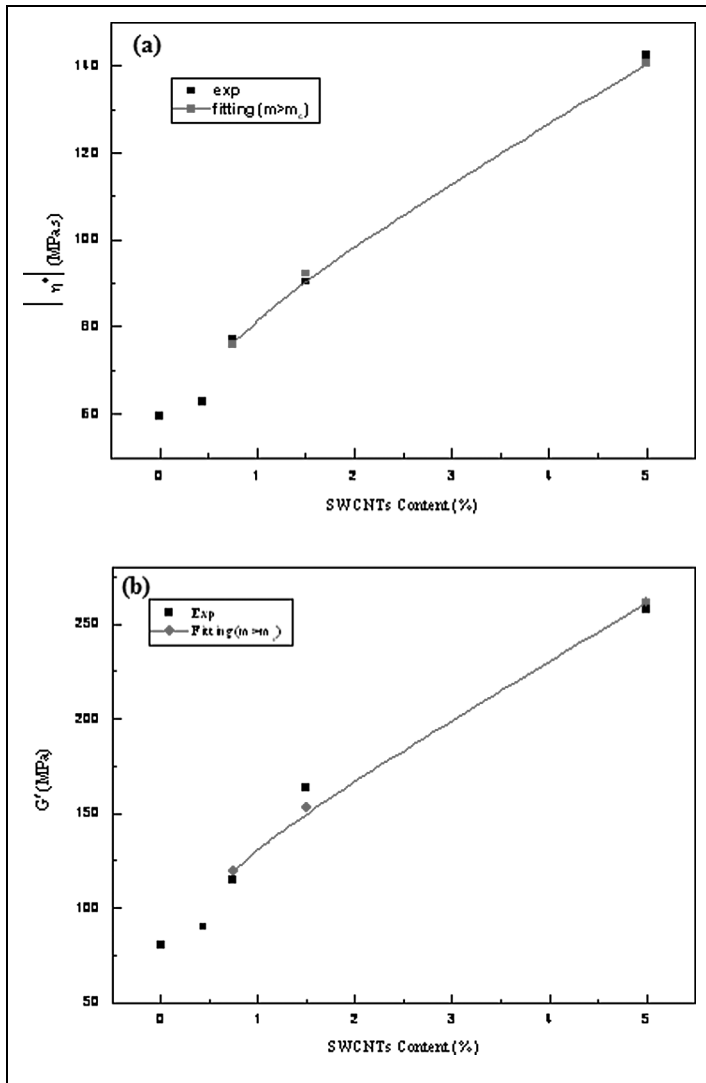


Figure 15. (a) Complex viscosity as a function of single-walled carbon nanotube (SWCNT) contents at 0.1 Hz. (b) Storage modulus as a function of SWCNT contents at 0.1 Hz.

observed in loss tangent and impedance results. This peak shifts isothermally toward higher frequency and the loss tangent value at the peak maximum decreases with increasing SWCNT loadings. Additionally, this study shows that the dielectric relaxation in SWCNT-P3OT composites is mainly due to the viscoelastic relaxation process. Rheological studies show that the complex viscosity $|\eta^*|$ decreases with increasing frequency, while both the storage modulus (G') and loss modulus (G'') of the SWCNT-P3OT

nanocomposites increase with increasing frequency, and this increment being more significant at low frequency. Rheological percolation threshold of SWCNTs in P3OT for both $|\eta^*|$ and G' was found at 0.5 wt%. Finally, there are strong evidences from the structure–property analysis that the addition of SWCNTs to P3OT host reduces the vibrational freedom of the polymer chains as a consequence of the intercalation of the polymer matrix into the nanotubes. Besides, at high level of SWCNTs loadings, the nanotubes form network-like structures in the P3OT host.

Acknowledgments

The authors acknowledge the King Abdelaziz City for Science and Technology (KACST), Saudi Arabia, for funding and providing the facilities required for this investigation.

References

1. Kim D-Y, Yun YS, Bak H, Cho SY and Jin H-J. Aspect ratio control of acid modified multi-walled carbon nanotubes. *Curr Appl Phys* 2010; 10: 1046–1052.
2. Sung J, Kim H, Jin H, Choi H and Chin I. Nanofibrous membranes prepared by multiwalled carbon nanotube/poly (methyl methacrylate) composites. *Macromolecules* 2004; 37: 9899–9902.
3. Xia B, Wang J, Wang X, Niu J, Sheng Z, Hu M, et al. Synthesis and application of graphitic carbon with high surface area. *Adv Funct Mater* 2008; 18: 1790–1798.
4. Kim HJ, Koizhaiganova RB, Karim MR, Lee GH, Vasudevan T and Lee MS. Synthesis and characterization of poly(3-octylthiophene)/single wall carbon nanotube composites for photovoltaic applications. *J Appl Polym Sci* 2010.
5. Lopezmata C, Nicho M, Hu H, Cadenaspiego G and Garciahernandez E. Optical and morphological properties of chemically synthesized poly3-octylthiophene thin films. *Thin Solid Films* 2005; 490: 189–195.
6. Tans S, Verschueren A and Dekker C. Room-temperature transistor based on a single carbon nanotube. *Nature* 1998; 393: 49–52.
7. Valentini L, Armentano I, Biagiotti J, Marigo A, Santucci S and Kenny J. AC conductivity of conjugated polymer onto self-assembled aligned carbon nanotubes. *Diam Relat Mater* 2004; 13: 250–255.
8. Ceronsolis J, Delarosa E and Penacabrera E. Absorption and refractive index changes of poly (3-octylthiophene) under NO₂ gas exposure. *Opt Mater* 2006; 29: 167–172.
9. Kazukauskas V, Pranaitis M, Cyras V, Sicot L and Kajzar F. Negative mobility dependence on electric field in poly(3-alkylthiophenes) evidenced by the charge extraction by linearly increasing voltage method. *Thin Solid Films* 2008; 516: 8988–8992.
10. Kline RJ and McGehee MD. Morphology and charge transport in conjugated polymers. *Polym Rev* 2006; 46: 27–45.
11. Koizhaiganova RB, Kim HJ, Vasudevan T and Lee MS. Double-walled carbon nanotube (DWCNT)–poly(3-octylthiophene) (P3OT) composites: Electrical, optical and structural investigations. *Synthetic Met* 2009; 159: 2437–2442.
12. Palacios-Lidón E, Perez-García B, Abellán J, Miguel C, Urbina A and Colchero J. Nanoscale characterization of the morphology and electrostatic properties of poly(3-octylthiophene)/graphite-nanoparticle blends. *Adv Funct Mater* 2006; 16: 1975–1984.
13. Spanggaard H. A brief history of the development of organic and polymeric photovoltaics. *Sol Energ Mat Sol C* 2004; 83: 125–146.

14. Valentini L, Armentano I, Biagiotti J, Frulloni E, Kenny J and Santucci S. Frequency dependent electrical transport between conjugated polymer and single-walled carbon nanotubes. *Diam Relat Mater* 2003; 12: 1601–1609.
15. Garai A, Kuila B, Samai S, Roy S, Mukherjee P and Nandi A. Physical and electronic properties in multiwalled carbon nanotube–poly (3 dodecylthiophene) nanocomposites. *J Polym Sci B: Polym Phys* 2009; 47: 1412–1425.
16. Koizhaiganova R, Kim H, Vasudevan T and Lee M. Double-walled carbon nanotube (DWCNT)-poly (3-octylthiophene)(P3OT) composites: Electrical, optical and structural investigations. *Synthetic Met* 2009; 159: 2437–2442.
17. Alexandrou I, Kymakis E and Amaratunga G. Polymer–nanotube composites: Burying nanotubes improves their field emission properties. *Appl Phys Lett* 2002; 80: 1435.
18. Kymakis E and Amaratunga G. Electrical properties of single-wall carbon nanotube-polymer composite films. *J Appl Phys* 2006; 99: 084302.
19. Kymakis E and Amaratunga G. Optical properties of polymer-nanotube composites. *Synthetic Met* 2004; 142: 161–167.
20. Murakami Y, Miyauchi Y, Chiashi S and Maruyama S. Direct synthesis of high-quality single-walled carbon nanotubes on silicon and quartz substrates. *Chem Phys Lett* 2003; 377: 49–54.
21. Borowiak-Palen E. Single-walled carbon nanotubes as nanotest tubes. *Phys Status Solidi B* 2007; 244: 4311–4314.
22. Huang Y, Li N, Ma Y, Du F, Li F, He X, et al.. The influence of single-walled carbon nanotube structure on the electromagnetic interference shielding efficiency of its epoxy composites. *Carbon*. 2007; 45: 1614–1621.
23. Ayes A. Dielectric relaxation and thermal stability of polycarbonate doped with $MnCl_2$ salt. *J Thermoplast Compos Mater* 2008; 21: 309.
24. Nguyen L, Hoppe H, Erb T, Günes S, Gobsch G and Sariciftci N. Effects of annealing on the nanomorphology and performance of poly (alkylthiophene): Fullerene bulk heterojunction solar cells. *Adv Funct Mater* 2007; 17: 1071–1078.
25. Dobrza ski L, Pawlyta M, Krzto A, Liszka B and Labisz K. Synthesis and characterization of carbon nanotubes decorated with platinum nanoparticles. *JAMME* 2010; 39: 184
26. Ayes A. Electrical and optical characterization of PMMA doped with $Y_0.0025Si_0.025Ba_0.9725$ (Ti (0.9) Sn0) O3 ceramic.
27. Ayes A. Dielectric properties of polyethylene oxide doped with NH_4I salt. *Polym J* 2009; 41: 616–621.
28. Ayes A and Abdel-Rahem R. Optical and electrical properties of polycarbonate/ $MnCl_2$ composite films. *J Plast Film Sheet* 2008; 24: 109.
29. Tanwar A, Gupta K, Singh P and Vijay Y. Dielectric parameters and ac conductivity of pure and doped poly (methyl methacrylate) films at microwave frequencies. *Bull Mater Sci* 2006; 29: 397–401.
30. Du F, Scogna R, Zhou W, Brand S, Fischer J and Winey K. Nanotube networks in polymer nanocomposites: rheology and electrical conductivity. *Macromolecules*. 2004; 37: 9048–9055.
31. Krishnamoorti R, Vaia R and Giannelis E. Structure and dynamics of polymer-layered silicate nanocomposites. *Chem Mater* 1996; 8: 1728–1734.
32. Ferry J. *Viscoelastic properties of polymers*. John Wiley, 1980.
33. Nalwa H. *Encyclopedia of nanoscience and nanotechnology*. California: American Scientific Publishers, 2004.
34. Krishnamoorti R and Giannelis E. Rheology of end-tethered polymer layered silicate nanocomposites. *Macromolecules* 1997; 30: 4097–4102.

35. Kim J and Kim S. Influence of multiwall carbon nanotube on physical properties of poly (ethylene 2, 6 naphthalate) nanocomposites. *J Polym Sci B: Polym Phys* 2006; 44: 1062–1071.
36. Larson R, Winey K, Patel S, Watanabe H and Bruinsma R. The rheology of layered liquids: lamellar block copolymers and smectic liquid crystals. *Rheol Acta* 1993; 32: 245–253.
37. Rosedale J and Bates F. Rheology of ordered and disordered symmetric poly (ethylenepropylene)-poly (ethylethylene) diblock copolymers. *Macromolecules* 1990; 23: 2329–2338.
38. Kulichikin V, Shumskii V and Semakov A. Rheological and relaxation behaviour of filled lc-thermoplastics and their blends. *Rheol Process Liquid Cryst Polym* 1996: 135.
39. Pötschke P, Fornes T and Paul D. Rheological behavior of multiwalled carbon nanotube/poly-carbonate composites. *Polymer* 2002; 43: 3247–3255.
40. Chatterjee T, Yurekli K, Hadjiev V and Krishnamoorti R. Single walled carbon nanotube dispersions in poly (ethylene oxide). *Adv Funct Mater* 2005; 15: 1832–1838.
41. Hu G, Zhao C, Zhang S, Yang M and Wang Z. Low percolation thresholds of electrical conductivity and rheology in poly (ethylene terephthalate) through the networks of multi-walled carbon nanotubes. *Polymer* 2006; 47: 480–488.
42. Pötschke P, Abdel-Goad M, Alig I, Dudkin S and Lellinger D. Rheological and dielectrical characterization of melt mixed polycarbonate-multiwalled carbon nanotube composites. *Polymer* 2004; 45: 8863–8870.